Published online 26 April 2017 *Nucleic Acids Research, 2017, Vol. 45, No. 11* **6923–6933**
doi: 10.1093/nar/gkx287

The *Streptomyces* master regulator BldD binds c-di-GMP sequentially to create a functional $BldD_2$-$(c\text{-}di\text{-}GMP)_4$ complex

Maria A. Schumacher[1,*], Wenjie Zeng[1], Kim C. Findlay[2], Mark J. Buttner[2], Richard G. Brennan[1] and Natalia Tschowri[3]

[1]Department of Biochemistry, Duke University School of Medicine, Durham, NC 27701, USA, [2]Department of Molecular Microbiology, John Innes Centre, Norwich Research Park, Norwich NR4 7UH, UK and [3]Institut für Biologie/Mikrobiologie, Humboldt-Universität zu Berlin, 10115 Berlin, Germany

Received February 20, 2017; Revised March 22, 2017; Editorial Decision April 10, 2017; Accepted April 12, 2017

ABSTRACT

Streptomyces **are ubiquitous soil bacteria that undergo a complex developmental transition coinciding with their production of antibiotics. This transition is controlled by binding of a novel tetrameric form of the second messenger, 3′-5′ cyclic diguanylic acid (c-di-GMP) to the master repressor, BldD. In all domains of life, nucleotide-based second messengers allow a rapid integration of external and internal signals into regulatory pathways that control cellular responses to changing conditions. c-di-GMP can assume alternative oligomeric states to effect different functions, binding to effector proteins as monomers, intercalated dimers or, uniquely in the case of BldD, as a tetramer. However, at physiological concentrations c-di-GMP is a monomer and little is known about how higher oligomeric complexes assemble on effector proteins and if intermediates in assembly pathways have regulatory significance. Here, we show that c-di-GMP binds BldD using an ordered, sequential mechanism and that BldD function necessitates the assembly of the $BldD_2$-$(c\text{-}di\text{-}GMP)_4$ complex.**

INTRODUCTION

Streptomyces are primarily soil-dwelling bacteria that have a complex developmental life cycle during which they transition from vegetative growth to a reproductive phase associated with the production of specialized aerial hyphae that differentiate into exospores for dispersion through a synchronized septation event (1–7). In addition to their fascinating developmental life cycle, *Streptomyces* are also notable as the most abundant source of antibiotics and other natural products used in medicine (8–10). Differentiation and antibiotic production are temporally and genetically coordinated, and so understanding the signals and mechanisms that initiate these processes is of significant interest. Extensive genetic analyses identified the regulators required for the initiation of development (2–7,11). These regulators are termed Bld (bald) because mutations in the corresponding genes prevent formation of the reproductive aerial hyphae that impart a 'fuzzy' appearance to colonies of the wild type. Subsequent studies showed that one Bld regulator, BldD, sits at the top of the developmental hierarchy, repressing the transcription of ∼170 sporulation genes during vegetative growth (4,5,11–15). Targets of BldD repression include most of the core transcriptional regulators that drive downstream developmental steps, as well as genes encoding critical components of the cell division and chromosome segregation machineries required for sporulation and septation (4,5,11,12). While BldD was known to be the master regulator of development, how its activity is controlled was only recently revealed when it was shown that it binds and is regulated by the second messenger 3′,5′-cyclic diguanylic acid (c-di-GMP) (16).

c-di-GMP was discovered as an allosteric effector of cellulose synthase in *Acetobacter xylinum* and subsequent studies revealed that it is one of the most widespread second messengers in bacteria (17,18). It is generated from two molecules of GTP by diguanylate cyclases (DGCs) that contain GGDEF domains (19–21) and degraded by phosphodiesterases (PDEs) characterized by EAL or HD-GYP domains (22–24). The diverse processes controlled by c-di-GMP include virulence, biofilm formation and motility (19,25–26). To date, effector proteins have been shown to bind c-di-GMP via degenerate active-site GGDEF/EAL motifs, GIL motifs, histidine kinase domains and PilZ domains (27–30). However, many c-di-GMP-binding effector proteins lack known c-di-GMP-binding motifs and must be discovered through functional studies. In addition to BldD, c-di-GMP-responsive transcription factors that have been identified through such analyses include

*To whom correspondence should be addressed. Tel: +1 919 684 9468; Fax: +1 919 684 8885; Email: maria.schumacher@duke.edu

the *Mycobacterium smegmatis* TetR-like activator LtmA, the *Pseudomonas aeruginosa* NtrC-type protein FleQ, the *Xanthomonas* CRP-FNR-like protein Clp, the *Burkholderia* Bcam1349 protein, *Vibrio cholerae* VpsR, *P. aeruginosa* BlrR and the FixJ-LuxR-CsgD family member VpsT (31–36). The 18 kDa BldD protein contains a unique C-terminal domain (CTD) in addition to its N-terminal helix-turn-helix (HTH) DNA-binding domain (14–16). Biochemical and structural studies revealed that this BldD domain binds an unprecedented tetrameric form of c-di-GMP, which glues together two otherwise non-interacting BldD CTD subunits (16). The resultant dimerized BldD binds its palindromic DNA sites and represses developmental progression. The structures revealed that BldD recognizes the c-di-GMP tetramer by a unique c-di-GMP signature sequence, RXD-X_8-RXXD, and biochemical assays confirmed the four c-di-GMP molecules: two BldD subunits stoichiometry observed in the structure (16). However, the tetrameric form of c-di-GMP observed in the $BldD_2$-$(c\text{-}di\text{-}GMP)_4$ structure is not found in solution. Indeed, c-di-GMP is mostly monomeric in solution at physiological concentrations and prior to studies on BldD, only monomers or intercalated c-di-GMP dimers had been observed in crystal structures of complexes with effector proteins (19,37–38).

Because the c-di-GMP tetramer bound by BldD has yet to be observed in solution, it is unclear how it assembles on the protein. The BldD binding motif has a bipartite nature, in which motif 1, composed of residues 114–116 (RGD) primarily interacts with one c-di-GMP intercalated dimer and motif 2, residues 125–128 (RQDD), interacts with the other c-di-GMP dimer (16). Motif 2 makes more contacts to the c-di-GMP molecules than does motif 1. However, Arg114 from motif 1 interacts with both c-di-GMP dimers and the nucleobases of the two c-di-GMP dimers also contact each other to stitch together the c-di-GMP tetramer. Thus, the c-di-GMP tetramer could assemble cooperatively with no intermediates or via a multistep process using a random or ordered sequential mechanism. Understanding this assembly process is key to delineating the precise mechanism by which c-di-GMP binding activates the function of BldD. To dissect this mechanism we carried out structural, biochemical and *in vivo* studies. The resulting data reveal that c-di-GMP binds BldD using an ordered sequential mechanism. The structure of a BldD assembly intermediate bound to one c-di-GMP dimer was captured and showed that the protein can still form dimers. A BldD(D116A) mutation trapped this half-loaded assembly intermediate, allowing assessment of its function. BldD(D116A) bound DNA more weakly than wild-type BldD, both *in vitro* and *in vivo*, and the *bldD D116A* mutant had a null phenotype, demonstrating that assembly of the fully complexed $BldD_2$-tetrameric c-di-GMP complex is required to regulate entry into development.

MATERIALS AND METHODS

Bacterial strains and plasmid construction

Strains, plasmids and oligonucleotides used are shown in Supplementary Table S1. BW25113 (39) containing a λ RED plasmid, pIJ790, was used to replace the kan^R marker on the PI1_D11 cosmid with the *apr-oriT* region amplified from the pIJ773 template plasmid. HME68 (40) was used for λ RED-mediated recombineering of the PI1_D11 *apr-oriT* cosmid with the single-strand oligonucleotide ssOligo bldD-D116A (Supplementary Table S1) to create the D116A mutation in the *bldD* locus on the cosmid. ET12567 containing pUZ8002 (41) was used for conjugation experiments. *S. venezuelae* strains (Supplementary Table S1) were grown at 30°C on maltose–yeast extract–malt extra ct (MYM) medium containing 50% tap water (MYM-TAP) and 200 μl trace element solution per 100 ml. Liquid cultures were grown under aeration at 250 rpm. Conjugations between *Escherichia coli* and *S. venezuelae* were carried out as previously described (42). For complementation, *bldD* and its promoter region were amplified using primers bldDSV–HindIII–pMS82-fw and bldDSV–KpnI–pMS82-rev listed in Supplementary Table S1 and cloned into HindIII–KpnI cut pMS82 to create pIJ10663. The plasmid was introduced into *S. venezuelae bldD* (D116A) by conjugation and the strain was named SVNT19. DNA fragments containing FL *bldD* (D116A) and *bldD* CTD(D116A) were produced synthetically and cloned into pET15b using NdeI and BamHI restriction sites by GenScript.

Generation of *S. venezuelae bldD* D116A mutant strain

Recombineering using single-strand oligonucleotide ssOligo bldD-D116A and *E. coli* HME68 strain was performed as described (43) to create the *bldD* (D116A) mutation on the PI1_D11 *kan*::*apr-oriT* cosmid. The mutagenized cosmid was confirmed by PCR and Sanger sequencing and introduced into *E. coli* ET12567/pUZ8002 for conjugation into *S. venezuelae*. Conjugation plates were incubated at room temperature (rt) overnight before overlaying with apramycin. Ex-conjugants were re-streaked once on plates containing apramycin and nalidixic acid and then several times on non-selective medium. The desired mutants arising from a double crossing over were screened for apramycin sensitivity followed by PCR to confirm the *bldD* (D116A) mutation. A PCR product comprising the complete *bldD* gene was sequenced and the resulting strain was named SVNT18.

DNA binding assays: EMSA and ChIP-seq experiments

DNA fragments spanning the *bldN* (141 bp) and *cdgB* (141 bp) promoter regions of *S. venezuelae* were generated by PCR using oligonucleotides listed in Supplementary Table S1. The binding reactions were performed using 0.3 μM His_6-BldD or His_6-BldD (D116A), 20 ng DNA and 0.5 μg poly[d(I-C)]. Different amounts of c-di-GMP (0.25 μM or 1.25 μM) were added to the mixture to assess affects on binding. Reaction mixtures were incubated for 20 min at rt and then run on a 5% polyacrylamide gel in 0.5 × TBE buffer followed by ethidium bromide staining. Chromatin immunoprecipitations were performed using an anti-BldD polyclonal antibody as previously described (16). ChIP-seq data have been deposited at ArrayExpress (E-MTAB-5328).

Cryo-scanning electron microscopy. Cryo-SEM was performed as previously described (44).

Purification of BldD CTD and BldD CTD mutants

To obtain protein for biochemical and structural studies, the region encoding the *S. venezuelae* BldD CTD domain (residues 80–166) was cloned into the pET15b vector. Initial protein expression of WT BldD CTD was carried out at 15°C overnight. Protein induction at this temperature resulted in high endogenous levels of c-di-GMP, as previously demonstrated (45–46). This c-di-GMP was bound by motif 2 in the BldD CTD, as later revealed in the structure. The presence of c-di-GMP in this BldD CTD protein was confirmed by A_{260}/A_{280} measurements of the protein samples, which indicated the significant presence of nucleic acid. Induction at 37°C for 2–3 h, significantly reduced or eliminated the contamination (45–46). Expressed BldD CTD protein was purified from the soluble cell lysate in one step via Ni-NTA affinity chromatography. Briefly, the BldD CTD cell lysate was loaded onto the Ni-NTA column and washed with five column volumes of buffer A (25 mM Tris pH 7.5, 300 mM NaCl, 5% glycerol) and eluted with 300 mM imidazole in buffer A. The hexa-histidine tag (his-tag) was removed using a thrombin capture cleavage kit. The BldD CTD(D128A) mutant was generated from the WT BldD CTD construct using QuikChange. This mutant and the BldD CTD(D116A) mutant protein were expressed and purified as per the WT protein. The proteins were concentrated in 10 kDa cutoff microcon filters, which also removed the cleaved his-tags. The his-tag free proteins were then utilized in fluorescence polarization (FP) and structural studies.

Size exclusion chromatographic analyses of BldD CTD(D116A)$_2$-(c-di-GMP)$_2$

Size exclusion chromatography experiments were carried out using a HiLoad 26/600 Superdex 75 pg column. BldD CTD(D116A) in the presence of 1 μM c-di-GMP at 0.9 mg/ml was loaded onto a column that had been pre-equilibrated with 300 mM NaCl, 5% glycerol, 20 mM Tris–HCl pH 7.5. The protein was eluted with one column volume at a rate of 1.5 ml/min at rt. The elution volume was plotted against a standard curve to determine the relative molecular weight. The standard curve was generated using aprotinin (6.5 kDa), cytochrome C (12.4 kDa), carbonic anhydrase (29 kDa) and albumin (66.5 kDa).

Crystallization and structure determination of WT BldD CTD$_2$-(c-di-GMP)$_2$ and BldD CTD(D116A)$_2$-(c-di-GMP)$_2$ complexes

All BldD CTD crystallizations were carried out at rt. Crystals of the WT *S. venezuelae* BldD CTD$_2$-(c-di-GMP)$_2$ complex were obtained using protein at 80 mg/ml via the hanging drop vapor diffusion method by mixing the protein 1:1 with 30% PEG 1500, 100 mM sodium acetate, pH 5.0. To crystallize the *S. venezuelae* BldD CTD(D116A)$_2$–(c-di-GMP)$_2$ complex the protein was concentrated to 40 mg/ml and c-di-GMP was added to a final concentration of 50 mM. Two crystal forms of this complex were obtained. Crystal form 1 was grown by mixing the complex 1:1 with a crystallization condition consisting of 1.6 M sodium/potassium phosphate, 100 mM Tris pH 7.5. Form 2 was produced by combining the complex 1:2 with a reagent consisting of 20% PEG 3000, 0.1 M sodium acetate pH 4.6, 0.1 M zinc chloride. To collect X-ray intensity data, the WT BldD CTD crystals were cryo-preserved by dipping a looped crystal in a solution consisting of the crystallization reagent supplemented with 20% glycerol and then placing the loop directly in the cryo-stream. These crystals take the space group $P6_1$ (Table 1). BldD CTD(D116A)$_2$–(c-di-GMP)$_2$ crystal form 1 was cryo-preserved from the drop while crystal form 2 was cryo-preserved by a quick dip in the crystallization solution containing 15% glycerol before placement in the cryo-stream. Collection of X-ray intensity data sets for all the crystals were carried out at beamline 8.3.1 at 100 K at the Advanced Light Source (ALS) and processed with MOSFLM (47). Phaser was used to solve the structures by molecular replacement (48) with one subunit of the BldD CTD structure as a search model (16). In each structure, after an initial round of refinement, c-di-GMP molecules were clearly visible and were manually fit into the density. Finally, solvent molecules were added (49). After multiple rounds of rebuilding (49) and refinement in Phenix (50) and model assessment in Molprobity, convergence was reached and the final models validated using MolProbity (51). See Table 1 for data collection and refinement statistics.

Fluorescence polarization (FP) binding of BldD CTD, BldD CTD(D116A) and BldD CTD(D128A) to 2′-Fluo-AHC-c-di-GMP

To measure c-di-GMP binding by BldD CTD, BldD CTD(D116A) and BldD CTD(D128A), 2′-*O*-(6-[fluoresceinyl]aminohexylcarbamoyl)-cyclic diguanosine monophosphate (F-c-di-GMP) was used as the fluoresceinated ligand. The conjugation of the fluor, via a nine atom spacer, to a 2′ hydroxyl groups of the c-di-GMP, does not interfere with BldD CTD binding (16). FP experiments were carried out at 25°C in a buffer consisting of 150 mM NaCl and 25 mM Tris–HCl pH 7.5, which contained 1 nM F-c-di-GMP. Increasing concentrations of BldD CTD, BldD CTD(D116A) or BldD CTD(D128A) were titrated into the reaction mixture to obtain the binding isotherms. The resulting data were plotted using KaleidaGraph and curves were fit to deduce binding affinities. Each binding experiment was performed in triplicate. To determine the binding stoichiometry of c-di-GMP to BldD CTD(D116A), the buffer and conditions were identical to those used in the FP binding affinity determination experiments except that the concentration of the c-di-GMP was increased to 16 μM, which is 10-fold above the K_d (by using a solution containing 1 nM F-c-di-GMP and 15.999 μM c-di-GMP) thereby ensuring stoichiometric binding. BldD CTD(D116A) was titrated into the binding solution and the graph of the resulting data shows a linear increase in the observed mP until saturation with c-di-GMP, after which the mP values showed no increase.

Table 1. Data collection and refinement statistics for *S. venezuelae* BldD CTD_2-(c-di-$GMP)_2$ intermediate structures

BldD CTD complex structure	WT BldD CTD-(c-di-$GMP)_2$	BldD CTD (D116A)-(c-di-$GMP)_2$ form 1	BldD CTD (D116A)-(c-di-$GMP)_2$ form 2
Pdb code	5TZD	5TZF	5TZG
Data collection			
Space group	$P6_1$	$P2_12_12_1$	$P4_122$
a, *b*, *c* (Å)	103.8, 103.8, 49.7	87.1, 93.1, 94.1	82.0, 82.0, 59.2
α, β, γ (°)	90.0, 90.0, 120.0	90.0, 90.0, 90.0	90.0, 90.0, 90.0
Resolution (Å)	93.8–1.75	66.2–2.40	59.1–2.50
R_{sym}[a]	0.049 (0.112)[b]	0.054 (0.320)	0.051 (0.158)
R_{pim}	0.026 (0.090)	0.034 (0.214)	0.023 (0.089)
R_{meas}	0.056 (0.144)	0.065 (0.387)	0.056 (0.183)
CC(1/2)	0.997 (0.978)	0.998 (0.908)	0.997 (0.974)
$<I / \sigma(I)>$	17.0 (5.1)	12.4 (3.6)	21.4 (6.5)
Completeness (%)	95.1 (79.5)	93.3 (68.3)	97.2 (97.1)
Redundancy	4.1 (2.1)	3.3 (3.0)	5.5 (5.5)
Wilson *B*-factor (Å^2)	18.1	29.1	46.5
Refinement			
Resolution (Å)	93.8–1.75	66.2–2.40	59.1–2.50
R_{work}/R_{free} (%)[c]	20.0/23.9	22.9/26.7	19.7/24.7
R.M.S. deviations			
Bond lengths (Å)	0.024	0.011	0.008
Bond angles (°)	2.30	1.10	1.40
B-ave, protein (Å^2)	33.0	60.5	55.1
B-ave, c-di-GMP (Å^2)	22.2	37.8	33.9
B-ave, solvent (Å^2)	35.1	48.0	52.0
Atom #, protein	4704	4822	2397
Atom #, c-di-GMP	276	368	136
Atom #, Solvent	340	171	29
Ramachandran analyses			
Favored (%)	98.6	95.7	97.3
Disallowed (%)	0.0	0.0	0.0

[a] $R_{sym} = \Sigma\Sigma|Ihkl - I_{hkl}(j)|/\Sigma I_{hkl}$, where I_{hkl} is observed intensity and $I_{hkl}(j)|$ is the final average value of intensity.
[b] Values in parentheses are for the highest resolution shell.
[c] $R_{work} = \Sigma||F_{obs}| - |F_{calc}||/\Sigma|F_{obs}|$ and $R_{free} = \Sigma||F_{obs}| - |F_{calc}||/\Sigma|F_{obs}|$; where all reflections belong to a test set of 5% randomly selected data.

RESULTS

Structure of a BldD-c-di-GMP structural intermediate

Previous structures of the *S. venezuelae* BldD C-terminal domain (CTD) bound to c-di-GMP revealed a tetrameric form of c-di-GMP sandwiched by two monomeric, non-interacting BldD CTD subunits (Figure 1A). To gain insight into the c-di-GMP binding assembly mechanism of BldD including any structural changes upon c-di-GMP binding, we attempted to obtain a high-resolution crystal structure of the apo *S. venezuelae* BldD CTD. For these studies, recombinant wild-type (WT) BldD CTD was expressed in *E. coli* at 15°C overnight and the protein purified via a single Ni-NTA affinity chromatography step (Materials and Methods). Crystals were obtained and the structure solved by molecular replacement (MR) to 1.75 Å resolution and refined to final R_{work}/R_{free} values of 20.0%/23.9% (Table 1; Materials and Methods). As observed in previous structures, the BldD CTD is composed of two (β–α–α) repeats followed by a short C-terminal helix (15,16). Unexpectedly, however, there was an intercalated c-di-GMP dimer complexed to the protein, giving rise to a BldD CTD_2-(c-di-$GMP)_2$ structure (Figure 1B; Supplementary Figure S1). Subsequently, we found that inducing BldD protein production in *E. coli* at 15°C overnight led to high levels of endogenous c-di-GMP production, which co-purified with BldD. Similar findings of c-di-GMP expression in *E. coli* were previously noted (45–46). By contrast, expressing BldD for 2 h in exponential phase at 37°C resulted in protein mostly free of bound c-di-GMP (45–46).

The BldD CTD_2-(c-di-$GMP)_2$ structure contains a similarly organized BldD CTD dimer as found in the BldD CTD_2-(c-di-$GMP)_4$ complex, whereby the monomeric BldD subunits are connected via bridging contacts to the second messenger (Figure 1A and B). Contacts to the c-di-GMP dimer in the BldD CTD_2-(c-di-$GMP)_2$ structure are provided by the same residues in motif 2 (residues 125–128) that contact one of the c-di-GMP dimers in the fully loaded WT BldD CTD_2-(c-di-$GMP)_4$ structure (Figure 1A and B; Supplementary Figure S2A). Indeed, the BldD CTD_2-(c-di-$GMP)_2$ structure appears to have captured an intermediate in the assembly pathway. Just as in the BldD CTD_2-(c-di-$GMP)_4$ structure, the Arg125 side chains from both BldD subunits in the BldD CTD_2-(c-di-$GMP)_2$ structure pack together and make base specific hydrogen bonds to the inner, consecutively arranged guanine bases. The Arg125 side chains also stack with the guanine bases at the outer edges of the c-di-GMP dimer (Supplementary Figure S2A). The latter guanine bases are read by hydrogen bonds from Asp128, which contacts the guanine N2 and N1 atoms (Figure 1A; Supplementary Figure S2A). These combined interactions ensure that BldD binds guanine and not adenine nucleotides while also discriminating against pyrimidine nucleotides, the bases of which are too small to enable these contacts. Superimpositions of the individual subunits of the BldD CTD_2-(c-di-$GMP)_2$ intermediate and the BldD

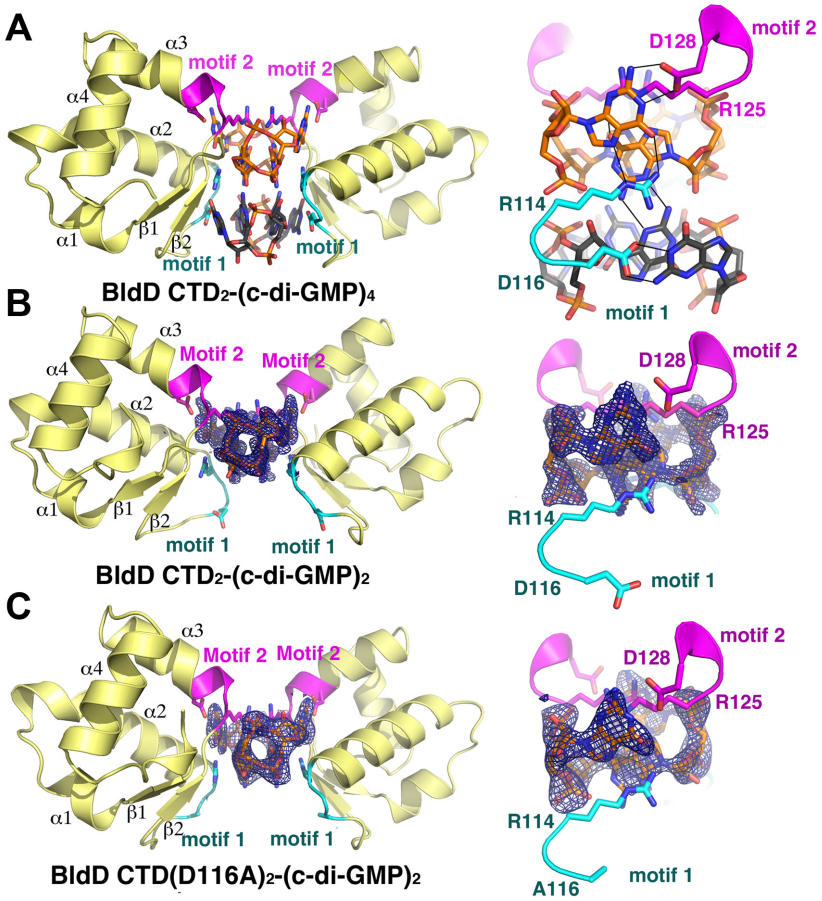

Figure 1. Comparison of the BldD CTD_2-$(c\text{-}di\text{-}GMP)_4$ structure with BldD CTD_2-$(c\text{-}di\text{-}GMP)_2$ intermediate structures. (**A**) Left, structure of the *S. venezuelae* BldD CTD_2-$(c\text{-}di\text{-}GMP)_4$ complex. Each subunit is labeled and motifs 1 and 2 are colored cyan and magenta, respectively. Right, key c-di-GMP contacting residues from these motifs, R114, D116, R125 and D128 are shown as atom-colored sticks. The bound c-di-GMP molecules are also shown as sticks with the c-di-GMP dimers bound in motif 1 and motif 2 colored gray and orange, respectively. (**B**) Left, 1.75 Å resolution structure of the *S. venezuelae* WT BldD CTD_2-$(c\text{-}di\text{-}GMP)_2$ intermediate complex with motifs 1 and 2 labeled as in Figure 1A. Right, close up view of the contacts to the c-di-GMP dimer and the $F_o - F_c$ map calculated from coordinates in which the c-di-GMP molecules were omitted, shown as a blue mesh. The map is contoured at 2.9σ. (**C**) Left, 2.40 Å resolution structure of the *S. venezuelae* BldD $CTD(D116A)_2$-$(c\text{-}di\text{-}GMP)_2$ complex with motifs 1 and 2 labeled as in Figure 1A. Right, close up of the contacts to the c-di-GMP and the $F_o - F_c$ map (blue mesh) calculated from coordinates in which the c-di-GMP molecules were omitted also shown. The map is contoured at 3.0σ.

CTD_2-$(c\text{-}di\text{-}GMP)_4$ structures results in root mean square deviations (rmsds) of 1.0–1.5 Å, indicating moderate structural divergence between the complexes. Further analysis showed that these differences are localized to residues 115–120, which encompass the unoccupied motif 1 (Supplementary Figure S2B). These residues are flexible in the intermediate structure as evidenced by their increased thermal parameters (B factors) compared to the BldD CTD_2-$(c\text{-}di\text{-}GMP)_4$ complex, in which these residues bind a second c-di-GMP dimer and are well ordered. Thus, motif 1 is likely only stabilized upon binding the second c-di-GMP dimer.

Trapping the BldD CTD_2-$(c\text{-}di\text{-}GMP)_2$ intermediate via mutagenesis

The BldD CTD_2-$(c\text{-}di\text{-}GMP)_2$ intermediate structure shows that motif 2 can interact with one c-di-GMP dimer, suggesting that c-di-GMP binding by BldD may be sequential with the first c-di-GMP dimer binding to motif 2 followed by the second binding to motif 1. Alternatively, the BldD CTD_2-$(c\text{-}di\text{-}GMP)_2$ structure may have captured c-di-GMP bound to motif 2 because binding at this site has a low off rate or binding to motif 1 has a high off rate. Thus, the half-loaded structure did not formally distinguish between random and sequential binding. To probe the binding mechanism further, we created mutations that would retain binding at one motif yet disable binding at the other motif. To prevent high affinity c-di-GMP binding to motif 1 we generated a D116A mutation, because the side chain of Asp116 functions solely in c-di-GMP binding to motif 1. Similarly, to prevent c-di-GMP binding to motif 2 we generated a D128A mutation, as Asp128 only makes contacts to the c-di-GMP bound to this motif (Figure 1A).

Crystallization trials were carried out on these mutant proteins in the presence of a large excess of c-di-GMP (50 mM). BldD CTD(D128A) did not yield crystals. However, two different crystal forms of the BldD CTD(D116A) protein were obtained in the presence of c-di-GMP. The structures were solved by molecular replacement to 2.40 Å (form 1) and 2.50 Å (form 2) resolution (Table 1) (Figure 1C;

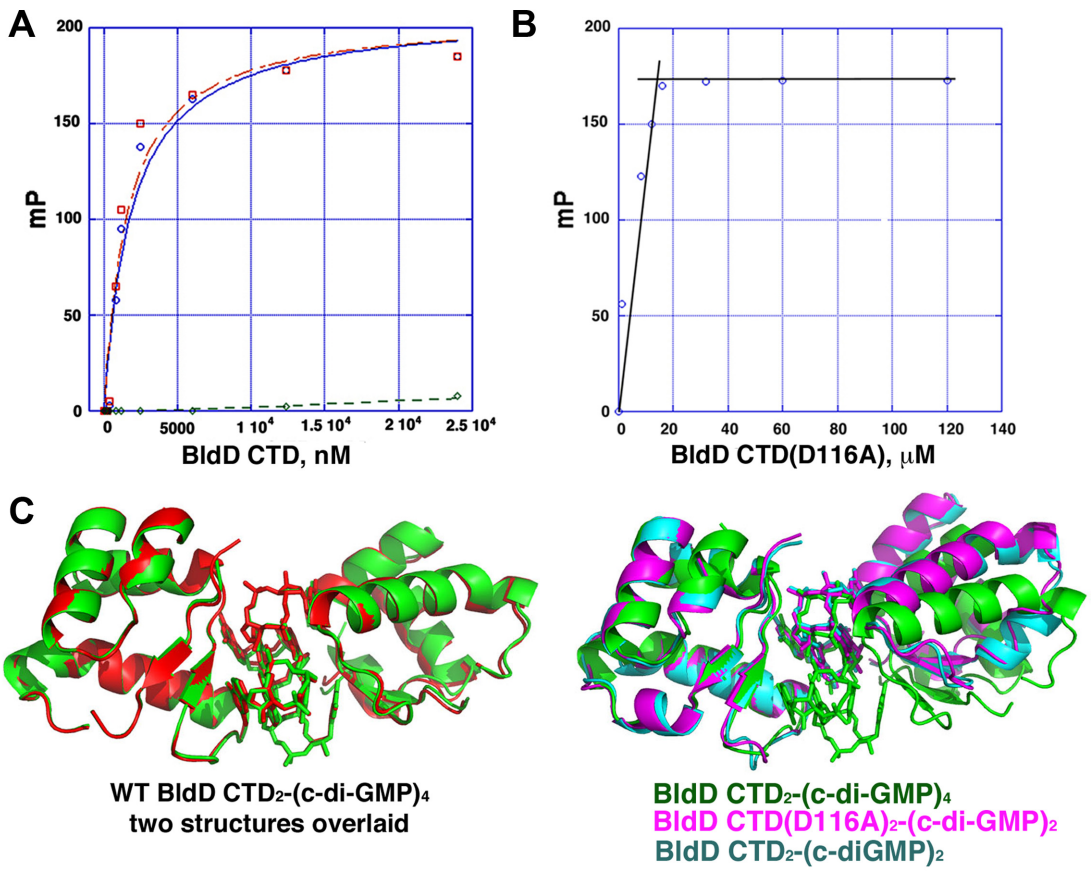

Figure 2. Structural and biochemical dissection of the BldD$_2$-(c-di-GMP)$_4$ assembly mechanism. (**A**) Representative fluorescence polarization (FP)-based isotherms of WT BldD CTD (blue), BldD CTD(D116A) (red) and BldD CTD(D128A) (green) binding to F-c-di-GMP. Notably, BldD CTD(D128A) shows essentially no c-di-GMP binding. The x and y axes correspond to BldD CTD concentration (nM) and millipolarization units (mP), respectively. (**B**) Determination of BldD CTD(D116A):c-di-GMP binding stoichiometry. For these experiments the c-di-GMP concentration was increased to 10-fold above the K_d (16 μM) to ensure stoichiometric binding. BldD CTD(D116A) was titrated into the binding solution and the graph of the resulting data shows a linear increase in the observed mP until saturation with c-di-GMP, after which the mP values showed no increase. The inflection point occurs at a BldD CTD(D116A) monomer concentration of ∼14 μM, which, when divided by the concentration of c-di-GMP (16 μM), indicates a stoichiometry of ∼1 BldD CTD(D116A) subunit to 1 c-di-GMP molecule. (**C**) Comparison of selected structures of the BldD CTD$_2$-(c-di-GMP)$_4$ complex (left) with BldD CTD$_2$-(c-di-GMP)$_2$ intermediates (right). In both cases, the leftmost subunits were superimposed to assess the relative juxtaposition of the remaining subunit in the dimer. The tetrameric c-di-GMP bound BldD subunits are anchored together and reveal only one dimer conformation. By contrast, the BldD-c-di-GMP intermediate structures appear more loosely attached and largely adopt a different dimer conformation. Neither the mutant nor wild type c-di-GMP dimer bound crystal forms take the wild type BldD CTD$_2$-(ci-di-GMP)$_4$ quaternary structure.

Supplementary Figures S1 and S3). Despite the high concentration of c-di-GMP used in these crystallizations, the BldD CTDs in both structures are bound only to a single c-di-GMP dimer via motif 2. Further, this c-di-GMP dimer is complexed in the same manner to motif 2 as the c-di-GMPs bound to the WT BldD CTD$_2$-(c-di-GMP)$_2$ intermediate and the c-di-GMP dimer bound at motif 2 in the fully loaded WT BldD CTD$_2$-(c-di-GMP)$_4$ structure (Figure 1).

BldD binds c-di-GMP using an ordered, sequential mechanism

The WT BldD CTD$_2$-(c-di-GMP)$_2$ and the BldD CTD(D116A)$_2$-(c-di-GMP)$_2$ structural studies support the notion that BldD binds c-di-GMP sequentially. However, to investigate the mechanism in more detail we carried out biochemical studies. To measure the binding affinities of mutant BldD proteins for c-di-GMP we employed fluorescence polarization (FP). The fluorescently labeled c-di-GMP analog, 2′-*O*-(6-[fluoresceinyl]aminohexylcarbamoyl)-cyclic diguanosine monophosphate (herein referred to as F-c-di-GMP) was used in these assays. F-c-di-GMP contains a fluorescein moiety attached to one of its 2′ ribose hydroxyls, which fortuitously does not interfere with BldD binding (16). The WT BldD CTD bound F-c-di-GMP with a K_d of ∼2 μM (1.8 ± 0.5 μM) (Figure 2A). The BldD CTD(D116A) mutant protein also showed robust c-di-GMP binding with a resultant K_d of 1.6 ± 0.5 μM. By contrast, the BldD CTD(D128A) protein interacted with F-c-di-GMP only at very high protein concentrations (K_d not determined) (Figure 2A).

Previous FP analyses revealed that the WT BldD CTD interacts with c-di-GMP with a stoichiometry of two BldD subunits to four c-di-GMP molecules (16). Using the same

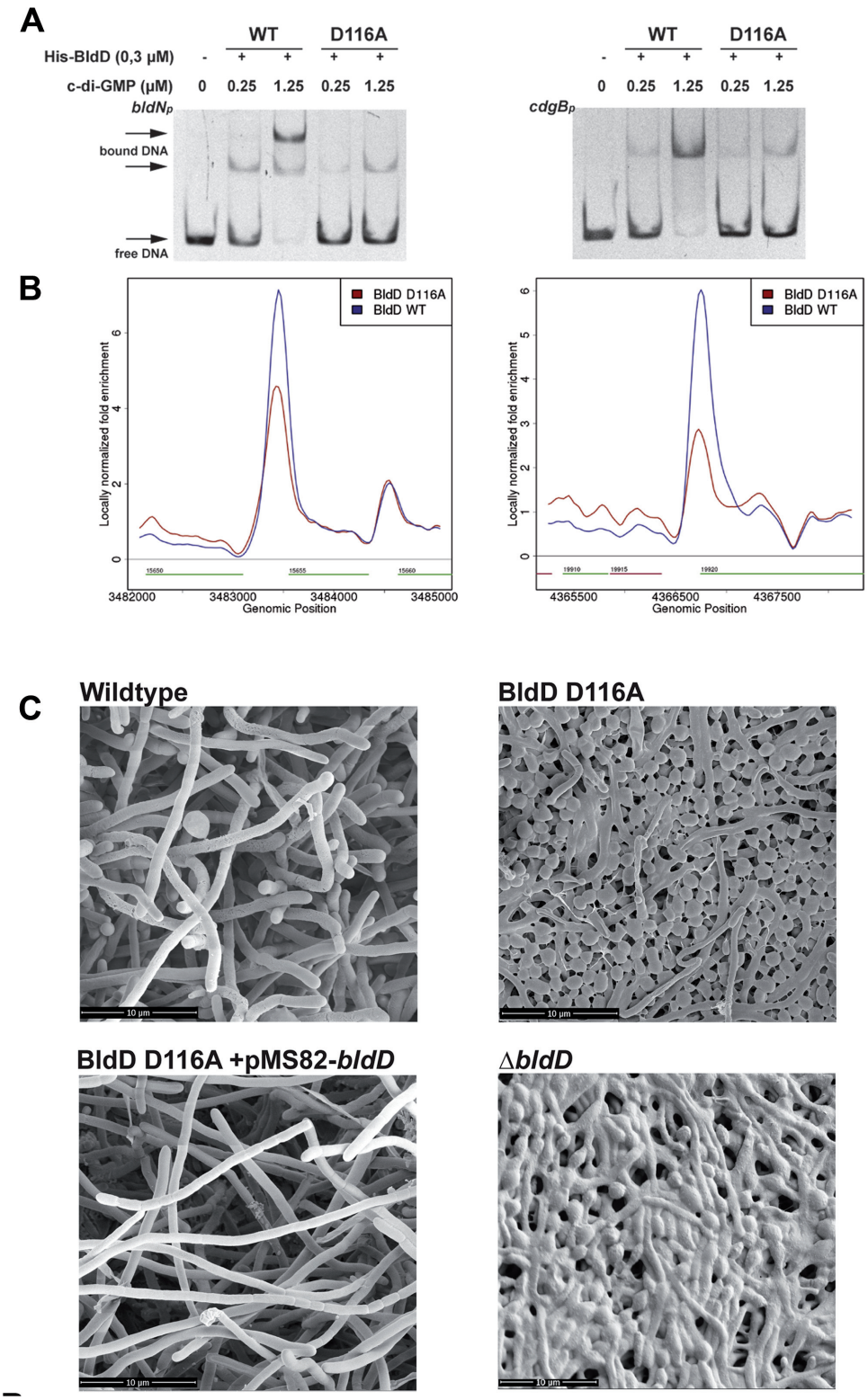

Figure 3. BldD(D116A) displays reduced binding to DNA and has a null phenotype. (**A**) EMSA analyses of BldD and BldD(D116A) binding to the *bldN* and *cdgB* promoters ± c-di-GMP. Free DNA and protein-DNA complexes (bound DNA) are indicated with arrows (**B**) *in vivo* BldD ChIP-seq data for the *bldN* and *cdgB* promoters. Color-coding of the ChIP samples is as follows: WT *S. venezuelae* (blue), *S. venezuelae bldD(D116A)* (red). Plots span ∼3 kb of DNA sequence. Genes running left to right are shown in green, and genes running right to left are shown in red. (**C**) Scanning electron micrographs (SEMs) showing, clockwise from the upper left, WT *S. venezuelae*, the *bldD(D116A)* mutant, the *ΔbldD* null mutant and the *bldD(D116A)* mutant complemented *in trans* from the ΦBT1 integration site (52,53). Strains were grown on MYM agar for 36 h at 30°C prior to imaging.

assay, we found that BldD CTD(D116A) bound c-di-GMP with a stoichiometry of two BldD CTD(D116A) to two c-di-GMP molecules, consistent with the crystal structures (Figures 1B, C and 2B). Thus, the combined structural and biochemical studies support an ordered, sequential mechanism in which c-di-GMP binds first to motif 2 of the BldD protein. These data also indicate that c-di-GMP binds to BldD sequentially as two c-di-GMP dimers. Previous studies revealed that c-di-GMP is mostly monomeric at physiological concentrations and only dimerizes at concentrations above 10 micromolar (37, 38). Such data would suggest that BldD binds c-di-GMP cooperatively as dimers within each motif. This would be consistent with the structures showing that residues in motifs 1 and 2 template binding of the intercalated dimer form of c-di-GMP (16). Arg114 is the only BldD residue that interacts with both c-di-GMP dimers (16). In the apo BldD CTD structure Arg114 is in a distinct orientation and largely disordered (15). Thus, it is notable that in the $BldD_2$-$(c\text{-}di\text{-}GMP)_2$ structure the Arg114 side chain adopts the same conformation as observed in the $BldD_2$-$(c\text{-}di\text{-}GMP)_4$ structure, indicating that this first binding event helps construct the second c-di-GMP dimer binding pocket in motif 1 (Supplementary Figure S4).

The BldD CTD_2-$(c\text{-}di\text{-}GMP)_2$ intermediate contains flexibly dimerized BldD subunits

BldD CTD structures in complex with tetrameric c-di-GMP form dimers that are locked into one specific conformation by the tetrameric c-di-GMP 'glue' (16) (Figure 2C). Indeed, these structures superimpose well across both CTD subunits (rmsds < 0.5 Å for all corresponding Cα atoms). By contrast, the BldD CTD_2-$(c\text{-}di\text{-}GMP)_2$ structures reported here, while also revealing BldD CTD dimers, show a range of dimer orientations with the CTD subunits appearing flexibly linked by the c-di-GMP molecules (Figure 2C). For example, comparison of the two BldD $CTD(D116A)_2$-$(c\text{-}di\text{-}GMP)_2$ structures shows that while individual CTD subunits overlay with rmsds of 0.3–0.4 Å (for all corresponding Cα atoms except residues 115–120), including both CTD subunits in superimpositions results in rmsds of 0.7–0.8 Å (Supplementary Figure S5). Interestingly, although the BldD CTD_2-$(c\text{-}di\text{-}GMP)_2$ and BldD $CTD(D116A)_2$-$(c\text{-}di\text{-}GMP)_2$ structures show a range of orientations between subunits, these 'dimers' are more similar to each other than the BldD CTD_2-$(c\text{-}di\text{-}GMP)_4$ form. Specifically, if one CTD subunit is overlaid, the remaining subunits show rotations of ∼5–7° in the intermediate structures while rotations of ∼20–25° are required to overlay CTDs of the BldD CTD_2-$(c\text{-}di\text{-}GMP)_2$ compared to the CTD_2-(c -di-GMP)$_4$ structure after one subunit is superimposed (Figure 2C). These findings suggest that the presence of a single c-di-GMP dimer between two BldD CTDs is not sufficient to form the stable $BldD_2$-$(c\text{-}di\text{-}GMP)_4$ dimer state and hence may not be functional as a repressor. Our BldD $CTD(D116A)_2$-$(c\text{-}di\text{-}GMP)_2$ structure showed that this mutant only binds c-di-GMP in motif 2, trapping this intermediate. Thus, the BldD(D116A) substitution provided a convenient tool to assess the competence of this assembly intermediate for DNA binding and its *in vivo* ability to restrain entry into development.

EMSA and ChIP studies on BldD$(D116A)_2$-$(c\text{-}di\text{-}GMP)_2$ intermediate

To compare DNA binding by WT BldD with that of BldD(D116A) we first employed electrophoretic shift mobility assays (EMSAs). These experiments analyzed the ability of these proteins to bind to the promoter regions of two well-characterized BldD target genes, *bldN,* which has two BldD operator binding sites (12), and *cdgB*, which harbors one BldD operator. WT BldD bound the target promoters with high affinity upon addition of c-di-GMP (0.25–1.25 μM) (Figure 3A). By contrast, the BldD(D116A) mutant displayed much weaker binding under identical conditions (Figure 3A). These data show that the c-di-GMP tetramer bound form of BldD is required for high affinity operator binding. Using a constructed *bldD(D116A)* mutant in which the D116A mutation was introduced into the *bldD* gene of WT *S. venezuelae* at the native locus, we next performed global BldD chromatin immunoprecipitation sequencing (ChIP-seq) analysis to examine DNA binding *in vivo* (Materials and Methods). Consistent with our EMSA studies, the ChIP-seq data showed that BldD(D116A) exhibited reduced occupancy of its *in vivo* binding sites compared to WT BldD (Figure 3B). Importantly, western blotting showed that the D116A mutation had no effect on BldD protein levels (Supplementary Figure S6).

BldD must be fully loaded with a c-di-GMP tetramer to mediate its function as a developmental regulator

Although the EMSA and ChIP analysis showed a significant reduction in target DNA binding by BldD(D116A), it remained unclear whether this level of DNA binding might be sufficient to enable the half-loaded $BldD_2$-$(c\text{-}di\text{-}GMP)_2$ intermediate to restrain entry into development. Thus, to assess the function of the half-loaded intermediate *in vivo*, we utilized the constructed *bldD*(D116A) mutant and analyzed its developmental phenotype (Materials and Methods). Strikingly, the *bldD*(D116A) mutant had a null phenotype. Like the congenic *bldD* deletion mutant (16), it produced small, soft, friable colonies devoid of aerial hyphae, and cryo scanning electron microscopy (cryo-SEM) showed that the biomass of even young (36 h) colonies of the *bldD*(D116A) mutant consisted almost entirely of spores, just like the null mutant (Figure 3C). The *bldD*(D116A) mutant was fully complemented in trans by a WT copy of *bldD* (Figure 3C). Thus, these data demonstrate that BldD must be fully loaded with a c-di-GMP tetramer to mediate its *in vivo* function as a developmental regulator.

BldD $CTD(D116A)_2$-$(\text{-}c\text{-}diGMP)_2$ does not form a stable dimer

The DNA binding and *in vivo* data unequivocally demonstrate that the BldD assembly intermediate, BldD CTD_2-$(c\text{-}di\text{-}GMP)_2$, is not active in mediating the physiological functions of BldD as a master regulator of development. However, crystals structures of the BldD intermediate showed that the protein can dimerize with just one c-di-GMP dimer bound to motif 2. However, while the c-di-GMP dimer bound to motif 2 mediates dimerization under the high protein concentrations found in crystals, this may not be the

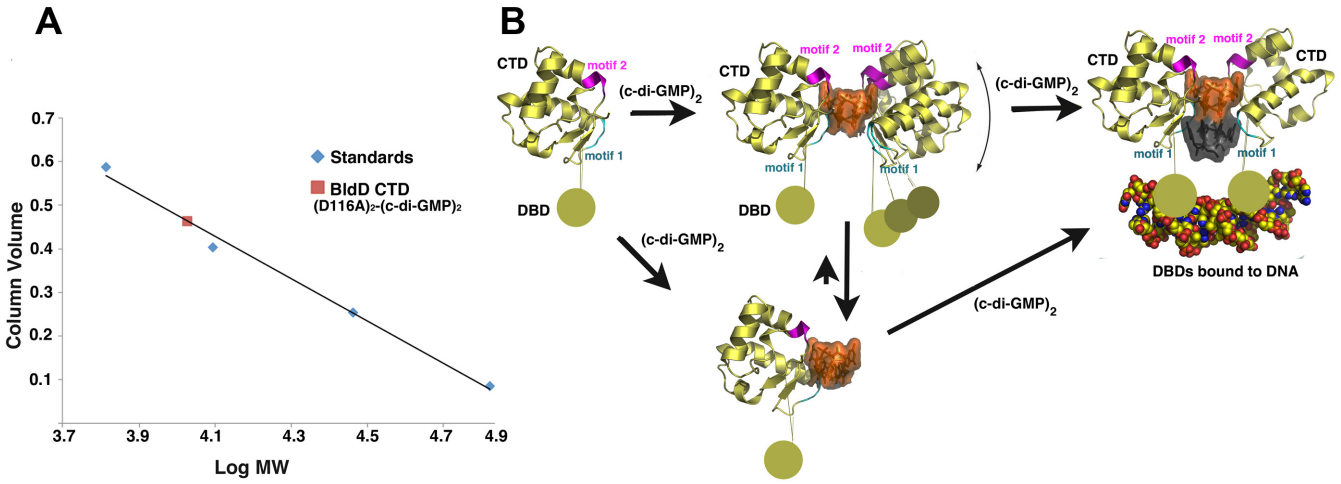

Figure 4. Molecular assembly mechanism of $BldD_2$-$(c\text{-}di\text{-}GMP)_4$. (**A**) Size exclusion chromatography (SEC) analysis of BldD CTD(D116A) in the presence of 1 μM c-di-GMP and a concentration of 0.9 mg/ml (labeled and shown as red square). The calculated molecular weight for the largest peaks (80–90% of the sample) is 11 kDa, consistent with a monomer of the BldD CTD. (**B**) Schematic molecular mechanism of tetrameric c-di-GMP assembly on BldD. At low c-di-GMP concentrations BldD exists as a monomer (motif 1 and motif 2 are colored cyan and magenta, respectively). Increasing intracellular concentrations of c-di-GMP lead to the first binding event where one c-di-GMP intercalated dimer (orange) binds BldD motif 2. Binding of this initial c-di-GMP dimer allows for the formation of weak BldD dimers at high concentrations. Due to the weak dimerization, this intermediate is not biologically active. Further increases in c-di-GMP levels leads to docking of the second c-di-GMP dimer between motifs 1 of two BldD molecules, effectively locking the dimer into one conformation and activating BldD to bind DNA. Arrow lengths indicate favored reaction direction. The DNA binding domains of BldD are shown as dark yellow circles.

case at lower concentrations, such as found *in vivo*. Thus to assess the oligomerization state of the BldD(D116A) protein in complex with c-di-GMP at low concentrations we performed size exclusion chromatography (SEC) experiments in the presence of c-di-GMP (Materials and Methods). The results showed that at low concentrations (0.9 mg/ml) this protein is in a monomer-dimer equilibrium with ∼80–90% in the monomer state (Figure 4A). In contrast, the WT BldD CTD forms a robust dimer (16). Thus, by analogy to weak and strong oligomers, the interface created by binding a single c-di-GMP dimer to BldD that is observed in crystal structures is not sufficient to drive dimerization under low protein concentrations and provides a molecular explanation for the requirement that BldD must be fully loaded with a c-di-GMP tetramer for biological activity (Figure 4B).

DISCUSSION

The second messenger c-di-GMP can adopt alternate oligomerization states to impart distinct functions, binding to effector proteins as a monomer, as an intercalated dimer, or in the case of BldD, as a tetramer. However, c-di-GMP is primarily monomeric at physiological concentrations in solution and little is known about how higher oligomeric nucleotide complexes assemble on effector proteins and importantly, if assembly pathway intermediates have regulatory roles. Here, we probed the assembly mechanism of the tetrameric form of c-di-GMP on BldD and found that it is formed using an ordered, sequential mechanism, with c-di-GMP dimers binding first to motif 2 (RXXD) and then to motif 1 (RXD). Our data also show that, although the intermediate state with a single c-di-GMP dimer bound enables interactions between BldD subunits, the interactions are not adequate to create a fully functional BldD dimer capable of effective DNA binding. Critically, *in vivo* studies showed that only the tetrameric c-di-GMP bound BldD is capable of controlling the *Streptomyces* developmental program.

BldD is present not just in *Streptomyces*, but in almost all sporulating actinomycetes, and in some actinomycete species BldD controls not only morphological differentiation, but also directly controls expression of antibiotics (8–10), showing that the developmental processes regulated by $BldD_2$-$(c\text{-}di\text{-}GMP)_4$ in actinomycetes extend to components of their commercially important secondary metabolism. Although actinomycete BldD homologs display low similarity in their CTDs (as low as 48% identity), the bipartite RXD–X_8–RXXD c-di-GMP-binding signature is perfectly conserved amongst all BldD proteins. Moreover, all sporulating actinomycetes also encode DGCs and PDEs and so must make and degrade c-di-GMP. These observations suggest that the ordered, sequential formation of a $BldD_2$–$(c\text{-}di\text{-}GMP)_4$ complex is likely to be a conserved mechanism used to control developmental as well as other key processes throughout the sporulating actinomycetes.

ACCESSION NUMBERS

Structure factor amplitudes and coordinates have been deposited in the RCSB protein data bank (RCSB PDB) under the accession codes 5TZD, 5TZF and 5TZG. The ChIP-seq data has been deposited with the ArrayExpress database under accession number E-MTAB-5328.

SUPPLEMENTARY DATA

Supplementary Data are available at NAR Online.

ACKNOWLEDGEMENTS

We thank Matt Bush and Leah Catchpole for processing the ChIP-seq samples and Govind Chandra for analyzing the resulting data. We would like to acknowledge the Advanced Light Source (ALS) beamlines 8.3.1 for data collection. The Berkeley Center for Structural Biology is supported in part by the National Institutes of Health, National Institute of General Medical Sciences, and the Howard Hughes Medical Institute. The Advanced Light Source is supported by the Director, Office of Science, Office of Basic Energy Sciences, of the U.S. Department of Energy under Contract No. DE-AC02-05CH11231. Beamline 8.3.1 at the ALS is operated by the University of California Office of the President, Multicampus Research Programs and Initiatives grant MR-15-328599 and Program for Breakthrough Biomedical Research, which is partially funded by the Sandler Foundation.

FUNDING

National Institutes of Health [GM115547 to M.A.S.]; BBSRC [BB/H006125/1 to M.J.B.]; BBSRC Institute Strategic Programme [BB/J004561/1 to the John Innes Centre]; DFG Emmy Noether-Programme [TS 325/1-1 to N.T.]; Duke University School of Medicine (to M.A.S. and R.G.B.). Funding for open access charge: NIH or Duke startup funds.

Conflict of interest statement. None declared.

REFERENCES

1. Flärdh,K., Richards,D.M., Hempel,A.M., Howard,M. and Buttner,M.J. (2009) Regulation of apical growth and hyphal branching in *Streptomyces*. *Curr. Opin. Microbiol.*, **15**, 737–743.
2. Flärdh,K. and Buttner,M.J. (2009) *Streptomyces* morphogenetics: dissecting differentiation in a filamentous bacterium. *Nat. Rev. Microbiol.*, **7**, 36–49.
3. McCormick,J.R. and Flärdh,K. (2012) Signals and regulators that govern *Streptomyces* development. *FEMS Microbiol. Rev.*, **36**, 206–231.
4. Tschowri,N. (2016) Cyclic dinucleotide-controlled regulatory pathways in *Streptomyces* species. *J. Bacteriol.*, **198**, 47–54.
5. Bush,M.J., Tschowri,N., Schlimpert,S., Flärdh,K. and Buttner,M.J. (2015) c-di-GMP signalling and the regulation of developmental transitions in streptomycetes. *Nat. Rev. Microbiol.*, **13**, 749–760.
6. McCormick,J.R. (2009) Cell division is dispensable but not irrelevant in *Streptomyces*. *Curr. Opin. Microbiol.*, **12**, 689–698.
7. Jakimowicz,D. and van Wezel,G.P. (2012) Cell division and DNA segregation in *Streptomyces*: how to build a septum in the middle of nowhere? *Mol. Microbiol.*, **85**, 393–404.
8. Hopwood,D.A. (2007) *Streptomyces in Nature and Medicine: The Antibiotic Makers*. Oxford University Press, NY.
9. Liu,G., Chater,K.F., Chandra,G., Niu,G. and Tan,H. (2013) Molecular regulation of antibiotic biosynthesis in *Streptomyces*. *Microbiol. Mol. Biol. Rev.*, **77**, 112–143.
10. van Wezel,G.P. and McDowall,K.J. (2011) The regulation of the secondary metabolism of *Streptomyces*: new links and experimental advances. *Nat. Prod. Rep.*,**28**,1311–1333.
11. den Hengst,C.D., Tran,N.T., Bibb,M.J., Chandra,G., Leskiw,B.W. and Buttner,M.J. (2010) Genes essential for morphological development and antibiotic production in *Streptomyces coelicolor* are targets of BldD during vegetative growth. *Mol. Microbiol.*, **78**, 361–379.
12. Elliot,M.A., Bibb,M.J., Buttner,M.J. and Leskiw,B.K. (2001) BldD is a direct regulator of key developmental genes in *Streptomyces coelicolor* A3(2). *Mol. Microbiol.*, **40**, 257–269.
13. Elliot,M.A. and Leskiw,B.K. (1999) The BldD protein from *Streptomyces coelicolor* is a DNA-binding protein. *J. Bacteriol.*, **181**, 6832–6835.
14. Kim,I.K., Lee,C.J., Kim,M.K., Kim,J.M., Kim,J.H., Kim,H.S., Cha,S.S. and Kang,S.O. (2006) Crystal structure of the DNA-binding domain of BldD, a central regulator of aerial mycelium formation in *Streptomyces coelicolor* A3(2). *Mol. Microbiol.*, **60**, 1179–1193.
15. Kim,J.M., Won,H.S. and Kang,S.O. (2014) The C-terminal domain of the transcriptional regulator BldD from *Streptomyces coelicolor* A3(2) constitutes a novel fold of winged-helix domains. *Proteins*, **82**, 1093–1098.
16. Tschowri,N., Schumacher,M.A., Schlimpert,S., Chinnam,N.B., Findlay,K.C., Brennan,R.G. and Buttner,M.J. (2014) Tetrameric c-di-GMP mediates effective transcription factor dimerization to control Streptomyces development. *Cell*, **158**, 1136–1147.
17. Ross,P., Weinhouse,H., Aloni,Y., Michaeli,D., Weinberger-Ohana,P., Mayer,R., Braun,S., de Vroom,E., van der Marel,G.A., van Broom,J.H. *et al.* (1987) Regulation of cellulose synthase in *Acetobacter xylinum* by cyclic diguanylic acid. *Nature*, **325**, 279–281.
18. Hengge,R. (2009) Principles of c-di-GMP signalling in bacteria. *Nat. Rev. Microbiol.*, **7**, 263–273.
19. Jenal,U., Reinders,A. and Lori,C. (2017) Cyclic di-GMP: second messenger extraordinaire. *Nat. Rev. Microbiol.*, doi:10.1038/nrmicro.2016.190.
20. Paul,R., Weiser,S., Amiot,N.C., Chan,C., Schirmer,T., Giese,B. and Jenal,U. (2004) Cell cycle-dependent dynamic localization of a bacterial response regulator with a novel di-guanylate cyclase output domain. *Genes Dev.*, **18**, 715–727.
21. Schirmer,T. (2016) C-di-GMP synthesis: structural aspects of evolution, catalysis and regulation. *J. Mol. Biol.*, **428**, 3683–701.
22. Christen,M., Christen,B., Folcher,M., Schauerte,A. and Jenal,U. (2005) Identification and characterization of a cyclic di-GMP-specific phosphodiesterase and its allosteric control by GTP. *J. Biol. Chem.*, **280**, 30829–30837.
23. Ryan,R.P., Fouhy,Y., Lucery,J.F., Crossman,L.C., Spiro,S., He,Y.W., Zhang,L.H., Heeb,S., Cámara,M., Williams,P. *et al.* (2006) Cell-cell signaling in *Xanthomonas campestris* involves an HD-GYP domain protein that functions in cyclic di-GMP turnover. *Proc. Natl. Acad. Sci. U.S.A.*, **103**, 6712–6717.
24. Schmidt,A.J., Ryjenkov,D.A. and Gomelsky,M. (2005) The ubiquitous protein domain EAL is a cyclic diguanylate-specific phosphodiesterase: enzymatically active and inactive EAL domains. *J. Bacteriol.*, **187**, 4774–4781.
25. Römling,U., Galperin,M.Y. and Gomelsky,M. (2013) Cyclic di-GMP: the first 25 years of a universal bacterial second messenger. *Microbiol. Mol. Biol. Rev.*, **77**, 1–52.
26. Chou,S-H. and Galperin,M.Y. (2016) Diversity of cyclic di-GMP-binding proteins and mechanisms. *J. Bacteriol.*, **198**, 32–46.
27. Amikam,D. and Galperin,M.Y. (2006) PilZ domain is part of the bacterial c-di-GMP binding protein. *Bioinformatics*, **22**, 3–6.
28. Navarro,M.V., De,N., Bae,N., Wang,Q. and Sondermann,H. (2009) Structural analysis of the GGDEF-EAL domain-containing c-di-GMP receptor FimX. *Structure*, **17**, 1104–1116.
29. Newell,P.D., Monds,R.D. and O'Toole,G.A. (2009) LapD is a bis-(3′,5′)-cyclic dimeric GMP-binding protein that regulates surface attachment by *Pseudomonas fluorescens* Pf0-1. *Proc. Natl. Acad. Sci. U.S.A.*, **106**, 3461–3466.
30. Qi,Y., Chuah,M.L., Dong,X., Xie,K., Luo,Z., Tang,K. and Liang,Z.X. (2011) Binding of cyclic diguanylate in the non-catalytic EAL domain of FimX induces a long-range conformational change. *J. Biol. Chem.*, **286**, 2910–2917.
31. Fazli,M., O'Connell,A., Nilsson,M., Niehaus,K., Dow,J.M., Givskov,M., Ryan,R.P. and Tolker-Nielsen,T. (2011) The CRP/FNR family protein Bcam1349 is a c-di-GMP effector that regulates biofilm formation in the respiratory pathogen *Burkholderia cenocepacia*. *Mol. Microbiol.*, **82**, 327–341.
32. Krasteva,P.V., Fong,J.C., Shikuma,N.J., Beyhan,S., Navarro,M.V., Yildiz,F.H. and Sondermann,H. (2010) *Vibrio cholerae* VpsT regulates matrix production and motility by directly sensing cyclic di-GMP. *Science*, **327**, 866–868.
33. Chin,K.H., Lee,Y.C., Tu,Z.L., Chen,C.H., Tseng,Y.H., Yang,J.M., Ryan,R.P., McCarthy,Y., Dow,J.M., Wang,A.H. *et al.* (2010) The cAMP receptor-like protein CLP is a novel c-di-GMP receptor

linking cell-cell signaling to virulence gene expression in *Xanthomonas campestris*. *J. Mol. Biol.*, **396**, 646–662.
34. Baraquet,C. and Harwood,C.S. (2013) Cyclic diguanosine monophosphate represses bacterial flagella synthesis by interacting with the Walker A motif of the enhancer-binding protein FleQ. *Proc. Natl. Acad. Sci. U.S.A.*, **110**, 18478–18483.
35. Chambers,J.R., Liao,J., Schurr,M.J. and Sauer,K. (2014) BrlR from *Pseudomonas aeruginosa* is a c-di-GMP responsive transcription factor. *Mol. Microbiol.*, **92**, 471–487.
36. Li,W. and He,Z.G. (2012) LtmA, a novel cyclic di-GMP-responsive activator, broadly regulates the expression of lipid transport and metabolism genes in *Mycobacterium smegmatis*. *Nucleic Acids Res.*, **40**, 11292–11307.
37. Zhang,Z., Kim,S., Gaffney,B.L. and Jones,R.A. (2006) Polymorphism of the signaling molecule c-di-GMP. *J. Am. Chem. Soc.*, **128**, 7015–7024.
38. Gentner,M., Allan,M.G., Zaehringer,F., Schirmer,T. and Grzesiek,S. (2012) Oligomer formation of the bacterial second messenger c-di-GMP: reaction rates and equilibrium constants indicate a monomeric state at physiological concentrations. *J. Am. Chem. Soc.*, **134**, 1019–1029.
39. Datsenko,K.A. and Wanner,B.L. (2000) One-step inactivation of chromosomal genes in *Escherichia coli* K-12 using PCR products. *Proc. Natl. Acad. Sci. U.S.A.*, **97**, 6640–6645.
40. Thomason,L., Court,D.L., Bubunenko,M., Costantino,N., Wilson,H., Datta,S. and Oppenheim,A. (2007) Recombineering: Genetic engineering in bacteria using homologous recombination, *Current Protocols in Molecular Biology*. John Wiley & Sons, Inc., Hoboken, pp. 1–24.
41. Paget,M.S., Chamberlin,L., Atrih,A., Foster,S.J. and Buttner,M.J. (1999) Evidence that the extracytoplasmic function sigma factor σ^E is required for normal cell wall structure in *Streptomyces coelicolor* A3(2). *J. Bacteriol.*, **181**, 204–211.
42. Bibb,M.J., Domonkos,Á., Chandra,G. and Buttner,M.J. (2012) Expression of the chaplin and rodlin hydrophobic sheath proteins in *Streptomyces venezuelae* is controlled by σ^{BldN} and a cognate anti-sigma factor, RsbN. *Mol. Microbiol.*, **84**, 1033–1049.
43. Costantino,N. and Court,D.L. (2003) Enhanced levels of λ Red-mediated recombinants in mismatch repair mutants. *Proc. Natl. Acad. Sci. U.S.A.*, **100**, 15748–15753.
44. Bush,M.J., Bibb,M.J., Chandra,G., Findlay,K.C. and Buttner,M.J. (2013) Genes required for aerial growth, cell division and chromosome segregation are targets of WhiA before sporulation in *Streptomyces venezuelae*. *mBio*, **4**, doi:10.1128/mBio.00684-13.
45. Sommerfeldt,N., Possling,A., Becker,G., Pesavento,C., Tschowri,N. and Hengge,R. (2009) Gene expression patterns and differential input into curli fimbriae regulation of all GGDEF/EAL domain proteins in *Escherichia coli*. *Microbiology*, **155**, 1318–1331.
46. Spangler,C., Böhm,A., Jenal,U., Seifert,R. and Kaever,V. (2010) A liquid chromatography mass spectrometry method for quantitation of cyclic di-guanosine monophosphate. *J. Microbiol. Methods*, **81**, 226–231.
47. Leslie,A.G. (2006) The integration of macromolecular diffraction data. *Acta Crystallogr. D. Biol. Crystallogr.*, **62**, 48–57.
48. Bunkóczi,G., Schols,N., McCoy,A.J., Oeffner,R.D., Adams,P.D. and Read,R.J. (2013) Phaser. MRage: automated molecular replacement. *Acta Crystallogr. D. Biol. Crystallogr.*, **69**, 2276–2286.
49. Emsley,P. and Cowtan,K. (2004) Coot: model-building tools for molecular graphics. *Acta Crystallogr. D. Biol. Crystallogr.*, **60**, 2126–2132.
50. Adams,P.D., Afonine,P.V., Bunkoczi,G., Chen,V.B., Davis,I.W., Echols,N., Headd,J.J., Hung,L.W., Kapral,G.J., Grosse-Kunstleve,R.W. *et al.* (2010) PHENIX: a comprehensive Phyton-based system for macromolecular structure solution. *Crystallogr. D. Biol. Crystallogr.*, **66**, 213–221.
51. Chen,V.B., Arendall,W.B. 3rd, Headd,J.J., Keedy,D.A., Immormino,R.M., Kapral,G.J., Murray,L.W., Richardson,J.S. and Richardson,D.C. (2010) MolProbity: all-atom structure validation for macromolecular crystallography. *Crystallogr. D. Biol. Crystallogr.*, **66**, 12–21.
52. Gregory,M.A., Till,R. and Smith,M.C. (2003) Integration site for *Streptomyces* phage phiBT1 and development of site-specific integrating vectors. *J. Bacteriol.*, **185**, 5320–5323.
53. Gust,B., Challis,G.L., Fowler,K., Kieser,T. and Chater,K.F. (2003) PCR-targeted *Streptomyces* gene replacement identifies a protein domain needed for biosynthesis of the sesquiterpene soil odor geosmin. *Proc. Natl. Acad. Sci. U.S.A.*, **100**, 1541–1546.